Timescales for radiation belt electron acceleration and loss due to resonant wave-particle interactions: 1. Theory

Danny Summers,[1] Binbin Ni,[1] and Nigel P. Meredith[2]

Received 19 April 2006; revised 9 November 2006; accepted 22 November 2006; published 13 April 2007.

[1] Radiation belt electrons can interact with various modes of plasma wave in their drift orbits about the Earth, including whistler-mode chorus outside the plasmasphere, and both whistler-mode hiss and electromagnetic ion cyclotron waves inside the plasmasphere. Electrons undergo gyroresonant diffusion in their interactions with these waves. To determine the timescales for electron momentum diffusion and pitch angle diffusion, we develop bounce-averaged quasi-linear resonant diffusion coefficients for field-aligned electromagnetic waves in a hydrogen or multi-ion (H^+, He^+, O^+) plasma. We assume that the Earth's magnetic field is dipolar and that the wave frequency spectrum is Gaussian. Evaluation of the diffusion coefficients requires the solution of a sixth-order polynomial equation for the resonant wave frequencies in the case of a multi-ion (H^+, He^+, O^+) plasma, compared to the solution of a fourth-order polynomial equation for a hydrogen plasma. In some cases, diffusion coefficients for field-aligned waves can provide a valuable approximation for diffusion rates for oblique waves calculated using higher-order resonances. Bounce-averaged diffusion coefficients for field-aligned waves can be evaluated generally in minimal CPU time and can therefore be profitably incorporated into comprehensive kinetic radiation belt codes.

Citation: Summers, D., B. Ni, and N. P. Meredith (2007), Timescales for radiation belt electron acceleration and loss due to resonant wave-particle interactions: 1. Theory, *J. Geophys. Res.*, *112*, A04206, doi:10.1029/2006JA011801.

1. Introduction

[2] The Earth's outer electron radiation belt ($3 < L < 7$) is highly variable, particularly during magnetic storms or other geomagnetically disturbed periods [e.g., *Paulikas and Blake*, 1979; *Baker et al.*, 1986, 1994, 1997; *Li et al.*, 1997; *Reeves et al.*, 1998; *Obara et al.*, 2000; *Miyoshi et al.*, 2003; *Miyoshi and Kataoka*, 2005]. Modeling the dynamics of energetic radiation belt electrons is of much current interest in space physics. In part, motivation for this interest is that relativistic (>1 MeV) electrons, which are generated during the recovery phase of some storms, pose a serious potential hazard to orbiting satellites [*Baker et al.*, 1998; *Baker*, 2001, 2002]. Relativistic electrons are also precipitated into the Earth's atmosphere where they change the electrical and chemical properties of the stratosphere and mesosphere [e.g., *Lastovicka*, 1996; *Callis et al.*, 1998]. By providing such a coupling between the magnetosphere and middle atmosphere, relativistic electron precipitation could therefore constitute an important link between solar activity and global climate variability.

[3] Wave-particle interactions play a fundamental role in radiation belt electron dynamics; see the reviews by *Gendrin* [2001], *Horne* [2002], and *Thorne et al.* [2005a]. Gyroresonant interactions are associated with high-frequency waves in the range $0.1\ \Omega_{O+} < \omega < 0.8\ |\Omega_e|$, where Ω_{O+} is the oxygen ion gyrofrequency and $|\Omega_e|$ is the electron gyrofrequency. Waves in this frequency range include whistler-mode chorus, plasmaspheric hiss, and electromagnetic ion cyclotron (EMIC) waves. Drift-resonant interactions are associated with ULF waves at lower frequencies of a few mHz. Energy diffusion due to cyclotron resonance with chorus waves is a viable mechanism for generating relativistic electrons (>1 MeV) in the outer zone during storms [*Summers et al.*, 1998, 2002, 2004a, 2004b; *Roth et al.*, 1999; *Summers and Ma*, 2000; *Horne et al.*, 2005a; *Thorne et al.*, 2005a; *Varotsou et al.*, 2005]. Radial (cross-L) diffusion driven by enhanced ULF waves has also been cited as an effective mechanism for generating stormtime relativistic electrons [*Hudson et al.*, 2001; *Elkington et al.*, 2003]. While radial diffusion is effective for energizing electrons outside geosynchronous orbit, there is evidence that an additional local acceleration mechanism (e.g., VLF chorus diffusion) is required to explain the observed relativistic electron flux increases in the region $3 < L < 5$ [e.g., *O'Brien et al.*, 2003; *Miyoshi et al.*, 2003, 2004; *Shprits and Thorne*, 2004; *Iles et al.*, 2006]. Both *Horne et al.* [2005b] and *Shprits et al.*

[1]Department of Mathematics and Statistics, Memorial University of Newfoundland, St. John's, Newfoundland, Canada.
[2]British Antarctic Survey, Natural Environment Research Council, Cambridge, UK.

0148-0227/07/2006JA011801

[2006a] demonstrated that ULF wave-driven radial diffusion could not explain the formation of the new radiation belt in the "slot" region following the 2003 Halloween storm. *Horne et al.* [2005b] and *Shprits et al.* [2006a] found that energy diffusion driven by whistler-mode waves could explain the gradual buildup of electron fluxes to energies of several MeV in this slot region normally devoid of energetic electrons. Gyroresonant interactions with whistler-mode chorus also provide a process for electron loss from the radiation belts. Electron cyclotron resonance with chorus can cause pitch angle scattering into the loss cone and subsequent loss to the atmosphere [*Horne and Thorne*, 2003; *Summers et al.*, 2005; *Thorne et al.*, 2005b]. EMIC waves and plasmaspheric hiss can also contribute to the scattering loss of radiation belt electrons [*Summers and Thorne*, 2003; *Albert*, 2003; *Summers et al.*, 2005; *Meredith et al.*, 2006]. Magnetopause shadowing, or other processes including radial diffusion, may additionally contribute to the loss of radiation belt electrons. A broad discussion of the issues of radiation belt electron transport, acceleration, and loss is provided collectively in the papers by *Li and Temerin* [2001], *Friedel et al.* [2002], *O'Brien et al.* [2003], *Green and Kivelson* [2004], *Green et al.* [2005], and *Thorne et al.* [2005a].

[4] It is clear from the literature that further work is needed to quantify electron acceleration and loss processes in the radiation belts. The aim of the present work and the companion paper [*Summers et al.*, 2007] is to apply quasi-linear diffusion theory to quantify cyclotron resonant interactions of radiation belt electrons with whistler-mode chorus, plasmaspheric hiss, and EMIC waves. We use quasi-linear theory to investigate the average properties of the cyclotron resonant diffusion process. Nonlinear effects including phenomena such as phase trapping are therefore not included and are beyond the scope of our investigation. *Summers* [2005] derived readily computable formulae for the quasi-linear diffusion coefficients for cyclotron resonance with field-aligned (R-mode or L-mode) electromagnetic waves. In order to determine the rates of momentum diffusion and pitch angle diffusion appropriate to the Earth's assumed dipole magnetic field, we carry out bounce-averaging of the diffusion coefficients due to *Summers* [2005], and we assume a Gaussian frequency spectrum for the waves. Whereas *Summers* [2005] presented detailed results only for a hydrogen plasma, here we consider the more general case of a multi-ion (H^+, He^+, O^+) plasma. Local diffusion coefficients are given in section 2. In section 3 we plot R-mode and L-mode wave dispersion curves, with corresponding minimum resonant energy curves. We also plot in section 3 examples of "resonance regions" which are regions in (kinetic energy, pitch angle)-space over which gyroresonance can take place. Evaluation of resonant quasi-linear diffusion coefficients requires calculation of the appropriate resonant wave frequencies. We discuss the determination of the resonant frequencies for R-mode or L-mode waves in a multi-ion (H^+, He^+, O^+) plasma in section 4. The bounce-averaged diffusion coefficients are derived in section 5. In section 6 we briefly discuss our results. In the accompanying paper [*Summers et al.*, 2007] we apply the results presented herein to evaluate radiation belt electron timescales for acceleration and loss due to gyroresonance with VLF chorus, ELF plasmaspheric hiss, and EMIC waves.

2. Quasi-Linear Diffusion Coefficients

[5] We assume an infinite, homogeneous, collisionless plasma immersed in a uniform, static magnetic field $\mathbf{B_0} = B_0\, \hat{\mathbf{e}}_\mathbf{z}$, in the presence of superposed electromagnetic waves. We use quasi-linear diffusion theory to describe the effects of the waves on the particles in terms of a kinetic equation for the gyrophase-averaged phase-space density Φ. Ensemble-averaging of the wave fields is carried out. The general, relativistic quasi-linear diffusion equation for Φ, in the limit of gyroresonant diffusion, can be written in the form [e.g., *Melrose*, 1980],

$$\frac{\partial \Phi}{\partial t} = \frac{1}{\sin\alpha}\frac{\partial}{\partial \alpha}\left(D_{\alpha\alpha}\ \sin\alpha\ \frac{\partial \Phi}{\partial \alpha}\right) + \frac{1}{\sin\alpha}\frac{\partial}{\partial \alpha}\left(D_{\alpha p}\ \sin\alpha\ \frac{\partial \Phi}{\partial p}\right) + \frac{1}{p^2}\frac{\partial}{\partial p}\left(p^2\ D_{p\alpha}\ \frac{\partial \Phi}{\partial \alpha}\right) + \frac{1}{p^2}\frac{\partial}{\partial p}\left(p^2\ D_{pp}\ \frac{\partial \Phi}{\partial p}\right), \tag{1}$$

where $D_{\alpha\alpha}$, $D_{\alpha p} = D_{p\alpha}$, and D_{pp} are the diffusion or Fokker-Planck coefficients which depend on the properties of the waves; $p = \gamma m_\sigma v$ is the momentum of the particle of species σ, rest mass m_σ and speed v; $\gamma = (1 - v^2/c^2)^{-1/2}$ is the Lorentz factor (c is the speed of light); α is the pitch angle of the particle, and t denotes time. In the present study we treat only the special case of electromagnetic waves propagating parallel or antiparallel to the background magnetic field $\mathbf{B_0}$. We assume that the R-mode ($s = 1$) and L-mode ($s = -1$) waves each have the Gaussian spectral density,

$$\tilde{W}_s(\omega) = \frac{|\Delta B_s|^2}{8\pi}\frac{1}{\rho}\frac{1}{\delta\omega}e^{-\left(\frac{\omega-\omega_m}{\delta\omega}\right)^2}, \tag{2}$$

with

$$\rho = \frac{\sqrt{\pi}}{2}\left[erf\left(\frac{\omega_m - \omega_1}{\delta\omega}\right) + erf\left(\frac{\omega_2 - \omega_m}{\delta\omega}\right)\right], \tag{3}$$

where ω_1 is the lower frequency limit, ω_2 is the upper frequency limit, ω_m is the frequency of maximum wave power, $\delta\omega$ is a measure of the bandwidth, and *erf* is the error function. The wave spectral density (2) has been normalized so that

$$\frac{|\Delta B_s|^2}{8\pi} = \int_{\omega_1}^{\omega_2}\tilde{W}_s(\omega)d\omega, \tag{4}$$

where $|\Delta B_s|$ is the mean wave amplitude.

[6] Following the study of *Summers* [2005], we can now express the diffusion coefficients for the particle species σ as follows:

$$D_{\alpha\alpha} = \frac{\pi}{2}\frac{1}{\rho}\frac{\Omega_\sigma^2}{|\Omega_e|}\frac{1}{(E+1)^2}\sum_s\sum_j \cdot \frac{R\left(1 - \frac{x_j\cos\alpha}{y_j\beta}\right)^2 |dx_j/dy_j|}{\delta x|\beta cos\alpha - dx_j/dy_j|}e^{-\left(\frac{x_j - x_m}{\delta x}\right)^2}, \tag{5}$$

$$\frac{D_{\alpha p}}{p} = -\frac{\pi}{2}\frac{1}{\rho}\frac{\Omega_\sigma^2}{|\Omega_e|}\frac{1}{\beta}\frac{\sin\alpha}{(E+1)^2}\sum_s\sum_j \cdot \frac{R\left(\frac{x_j}{y_j}\right)\left(1-\frac{x_j\cos\alpha}{y_j\beta}\right)|dx_j/dy_j|}{\delta x|\beta\cos\alpha - dx_j/dy_j|}e^{-\left(\frac{x_j-x_m}{\delta x}\right)^2}, \quad (6)$$

$$\frac{D_{pp}}{p^2} = \frac{\pi}{2}\frac{1}{\rho}\frac{\Omega_\sigma^2}{|\Omega_e|}\frac{1}{\beta^2}\frac{\sin^2\alpha}{(E+1)^2}\sum_s\sum_j \cdot \frac{R\left(\frac{x_j}{y_j}\right)^2|dx_j/dy_j|}{\delta x|\beta\cos\alpha - dx_j/dy_j|}e^{-\left(\frac{x_j-x_m}{\delta x}\right)^2}, \quad (7)$$

where we have introduced the dimensionless variables,

$$x = \frac{\omega}{|\Omega_e|}, \quad y = \frac{ck}{|\Omega_e|} \quad (8)$$

and E is the dimensionless particle kinetic energy given by $E = E_k/(m_\sigma c^2) = \gamma - 1$; $\beta = v/c = [E(E + 2)]^{1/2} / (E + 1)$; $|\Omega_e| = e|B_0|/ (m_e c)$ is the nonrelativistic electron gyrofrequency, where e is the unit charge; $\Omega_\sigma = q|B_0|/ (m_\sigma c)$ is the nonrelativistic particle gyrofrequency where q is the particle charge; $R = |\Delta B_s|^2/B_0^2$ is the ratio of the energy density of the turbulent magnetic field to that of the background field, i.e., the relative wave power; $x_m = \omega_m/|\Omega_e|$, $\delta x = \delta\omega/|\Omega_e|$; and the derivative $dx_j/dy_j = dx(y_j)/dy$ is determined from the appropriate dispersion relation. In (5)–(7) the summations are carried out over the wave modes specified by $s = 1$ (R-mode) and $s = -1$ (L-mode), and over the resonant roots ω_j, k_j corresponding to each wave mode. As well as satisfying the relevant dispersion equation, the resonant frequency ω_j and corresponding resonant wave number k_j (where $j = 1, 2, \ldots, N$) satisfy the Doppler gyroresonance condition, which, for electrons or protons, can be expressed as

$$y = \frac{x + a}{\beta\cos\alpha}, \quad (9)$$

where

$$a = \frac{s\lambda}{\gamma}. \quad (10)$$

Here, $\lambda = -1$ corresponds to electrons and $\lambda = \varepsilon$ to protons, with $\varepsilon = m_e/m_p$, where m_e is the electron rest mass and m_p the proton rest mass. As in the work of *Summers* [2005], we restrict the wave frequency ω_j to be always positive, and we take a positive wave number ($k_j > 0$) to represent a forward propagating wave and negative wave number ($k_j < 0$) to represent a backward wave.

[7] The classical theory of waves in a uniform cold plasma is given, for instance, by *Stix* [1992]. The dispersion relations for R-mode ($s = 1$) or L-mode ($s = -1$) waves propagating parallel or antiparallel to a uniform magnetic field in a cold, multi-ion (H^+, He^+, O^+) plasma are

$$\frac{y^2}{x^2} = 1 + \frac{1}{\alpha^* x}\left(\frac{1}{s-x} - \frac{\varepsilon\eta_1}{x+s\varepsilon} - \frac{\varepsilon\eta_2}{4x+s\varepsilon} - \frac{\varepsilon\eta_3}{16x+s\varepsilon}\right), \quad (11)$$

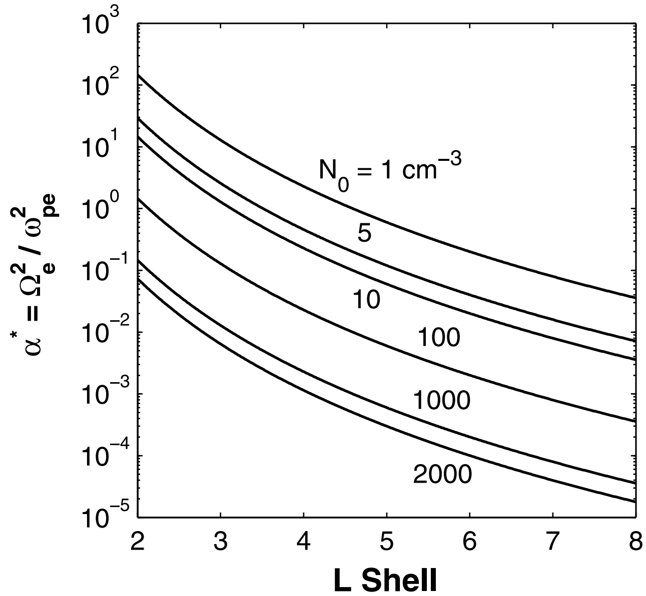

Figure 1. Equatorial variation of the parameter α^* with L, from (15), for a dipole geomagnetic field, for specified values of the electron number density N_0.

where

$$\alpha^* = \Omega_e^2/\omega_{pe}^2 \quad (12)$$

is a cold-plasma parameter; $\omega_{pe} = (4\pi N_0 e^2/m_e)^{1/2}$ is the electron plasma frequency where N_0 is the electron number density; $\eta_1 = N_1/N_0$, $\eta_2 = N_2/N_0$, and $\eta_3 = N_3/N_0$, where N_1, N_2 and N_3 denote the hydrogen (H^+), helium (He^+), and oxygen (O^+) ion number densities, respectively. The fractional ion compositions satisfy $\eta_1 + \eta_2 + \eta_3 = 1$, by charge neutrality. In the special case of a hydrogen plasma ($\eta_1 = 1$, $\eta_2 = \eta_3 = 0$), equations (11) reduce to the form,

$$\frac{y^2}{x^2} = 1 - \frac{b}{(x-s)(x+s\varepsilon)}, \quad (13)$$

where

$$b = (1+\varepsilon)/\alpha^*. \quad (14)$$

The parameter α^*, defined by (12), plays an important role in cold-plasma theory and can be written as $\alpha^* = 9.722 \times 10^{-6}B_0^2/N_0$, with B_0 (nT) and N_0 (cm^{-3}). If we adopt the Earth's equatorial dipole value for B_0, namely $B_0 = 3.12 \times 10^4/L^3$ (nT), then α^* can be expressed as

$$\alpha^* = \frac{9.464 \times 10^3}{L^6 N_0}, \quad (15)$$

with N_0 (cm^{-3}). In Figure 1 we plot α^*, given by (15), for a range of N_0 - values. In Figure 2 we use (15) to plot characteristic profiles of α^*, as a function of L, both inside and outside the plasmasphere, with the plasmapause boundary taken to be at $L = 3$. In the top of Figure 2, in order to represent "nominal" density values, we set $N_0 = 10$ cm^{-3} outside the plasmasphere and $N_0 = 10^3$ cm^{-3} inside the plasmasphere. In the bottom we use the "trough" density model of *Sheeley et al.* [2001], i.e., $N_0 = 124\ (3/L)^4$ cm^{-3},

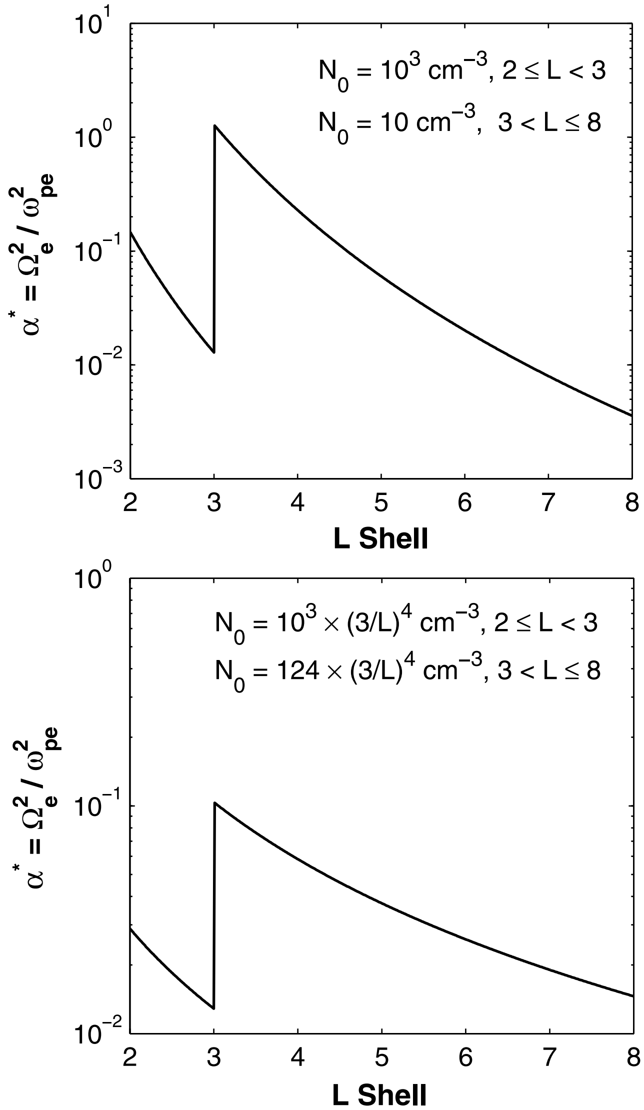

Figure 2. Equatorial profiles of the parameter α^* for a dipole geomagnetic field, with the plasmapause boundary located at $L = 3$. Assumed density N_0 profiles inside ($2 \le L < 3$) and outside ($3 < L \le 8$) the plasmasphere are specified in the top and bottom.

outside the plasmasphere, and we adopt a saturated density variation, $N_0 \propto L^{-4}$, inside the plasmasphere.

[8] The resonant roots x_j, y_j occurring in formulae (5)–(7) are solutions of the simultaneous equations (9) and (11) in the case of a multi-ion (H^+, He^+, O^+) plasma, or equations (9) and (13) for a hydrogen plasma. We defer discussion of the calculation of the roots x_j, y_j until section 4.

[9] It is possible that a singularity can occur in the diffusion coefficients (5)–(7) if the condition $\beta \cos \alpha = dx/dy$ is satisfied at a resonance. This is equivalent to the condition that the parallel speed of the particle equals the group speed of the wave. A point at which such a singularity occurs is called a critical point [see *Summers*, 2005]. The reader is referred to *Summers* [2005] for a discussion of critical values in the case of a hydrogen plasma. We do not discuss critical values further in the present paper.

[10] It should be noted that the definitions of $D_{\alpha\alpha}$ and $D_{\alpha p} = D_{p\alpha}$ used by *Summers* [2005] and also in the present paper differ, for instance, from those of *Lyons* [1974] and *Horne et al.* [2005a]. Specifically, the diffusion rates $D_{\alpha\alpha}$ and $|D_{\alpha p}|/p$ herein correspond respectively to the results $D_{\alpha\alpha}/p^2$ and $|D_{\alpha p}|/p^2$ given by *Lyons* [1974] and *Horne et al.* [2005a].

3. Dispersion Curves, Minimum Resonant Energy Curves, and (E_k, α) Resonance Regions

[11] The dispersion relations for R-mode ($s = 1$) or L-mode ($s = -1$) waves are given by equation (13) for a hydrogen plasma and by (11) for a multi-ion (H^+, He^+, O^+) plasma. We plot a selection of dispersion curves in the top of Figures 3–6 for a range of values of the parameter $\alpha^* =$

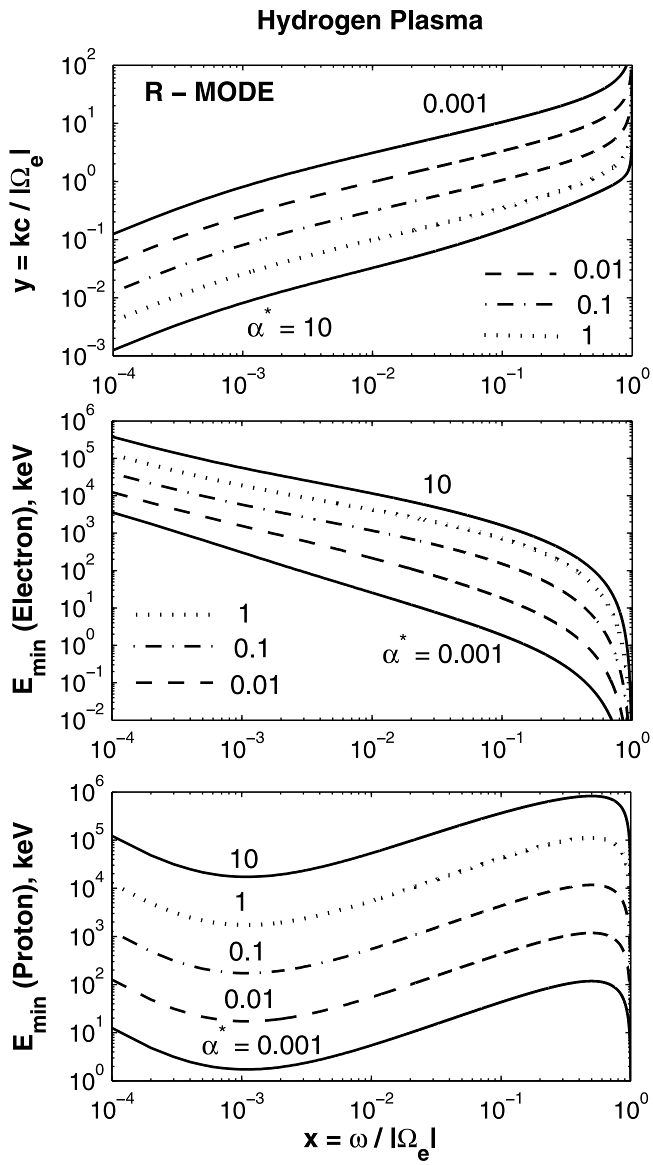

Figure 3. R-mode dispersion curves for a hydrogen plasma for specified values of $\alpha^* = \Omega_e^2/\omega_{pe}^2$ (top). Corresponding minimum resonant energy profiles for electrons (middle) and protons (bottom).

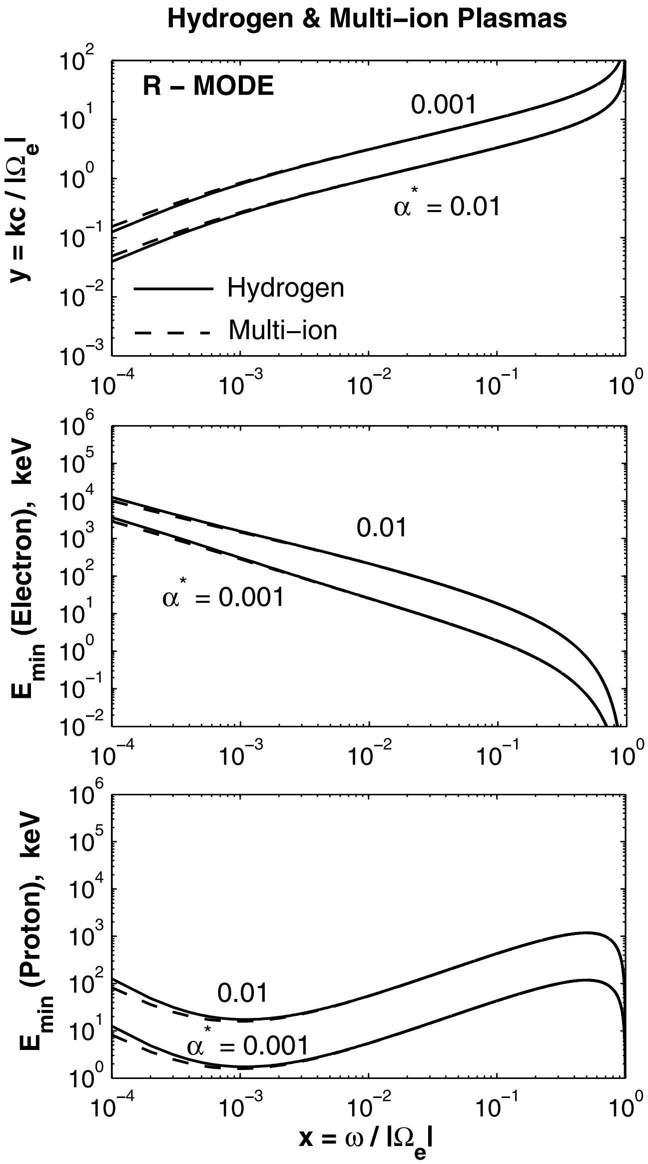

Figure 4. Comparison of R-mode dispersion curves in a hydrogen plasma and multi-ion (H^+, He^+, O^+) plasma for specified α^*-values (top). Corresponding minimum resonant energy profiles for electrons (middle) and protons (bottom). Fractional ion number densities are $\eta_1 = 0.75$, $\eta_2 = 0.2$, $\eta_3 = 0.05$.

Ω_e^2/ω_{pe}^2. In Figure 3 we plot dispersion curves for R-mode waves in a hydrogen plasma. In Figure 4, comparison of the dispersion curves for R-mode waves in hydrogen and multi-ion (H^+, He^+, O^+) plasmas demonstrates that inclusion of additional ions has negligible effect, except possibly at very small frequencies. For L-mode waves, however, inclusion of additional ions changes the basic dispersion properties. Specifically, L-mode waves propagate in a single band in a hydrogen plasma (Figure 5), but in three separate bands in a multi-ion (H^+, He^+, O^+) plasma (Figure 6). In Figure 6 we show L-mode dispersion curves for three different sets of values of the ion composition (η_1, η_2, η_3) to illustrate that the fractional ion composition can sensitively influence the dispersion relation. As shown in Figures 3–6, in all cases, the dispersion curves are strongly influenced by the value of the cold plasma parameter $\alpha^* = \Omega_e^2/\omega_{pe}^2$.

[12] Detailed examination of the gyroresonance condition (9) reveals that for a given value of α^* and for waves of a particular mode and frequency, there exists a minimum value of the particle kinetic energy $E_{\min}$ for which gyroresonant wave-particle interaction can take place. Here we develop formulae for $E_{\min}$ for both electrons and protons, each in resonance with either R-mode or L-mode waves. If $v_\parallel$, $v_\perp$ denote the components of particle velocity parallel and perpendicular to $\mathbf{B_0}$, where $v^2 = v_\parallel^2 + v_\perp^2$, then the gyroresonance condition (9), expressed in terms of $v_\parallel$ and $v_\perp$, is represented by an ellipse, the "resonance ellipse," in ($v_\parallel$, $v_\perp$)-space. From the resonance ellipse, it is straightforward to deduce that the minimum particle energy for which gyroresonant wave-particle interaction can take place is found by setting $v_\perp = 0$ in the resonance condition. We find

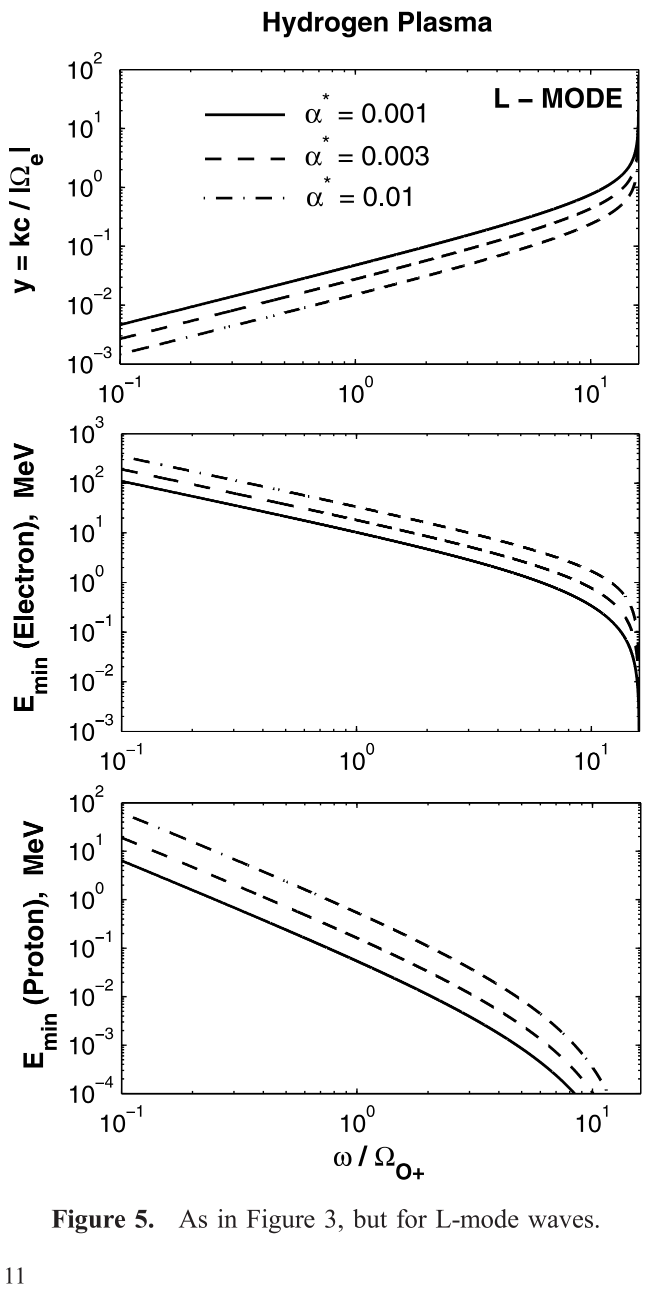

Figure 5. As in Figure 3, but for L-mode waves.

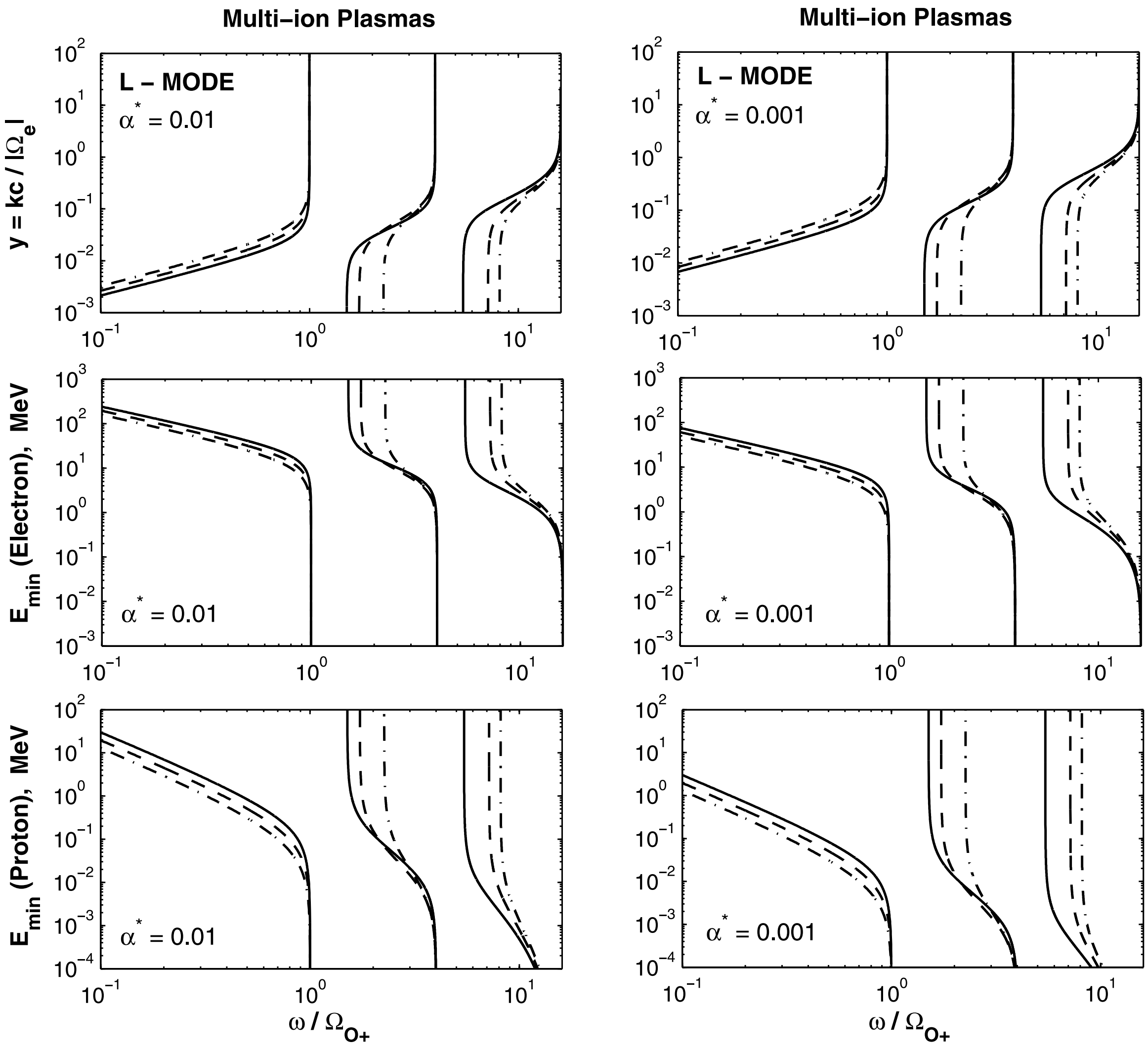

Figure 6. L-mode dispersion curves for multi-ion (H^+, He^+, O^+) plasmas for specified α^* - values (top). Corresponding minimum resonant energy profiles for electrons (middle) and protons (bottom). Fractional ion number densities are $\eta_1 = 0.85$, $\eta_2 = 0.1$, $\eta_3 = 0.05$ (solid curves); $\eta_1 = 0.7$, $\eta_2 = 0.2$, $\eta_3 = 0.1$ (dashed); $\eta_1 = 0.6$, $\eta_2 = 0.2$, $\eta_3 = 0.2$ (dot-dashed).

that the minimum resonant energy for electrons ($\sigma = e$) or protons ($\sigma = p$) can be written

$$E_{\min} = \frac{(E_k)_{\min}}{m_\sigma c^2} = \gamma_{\min} - 1 = \left[1 - \frac{(v_\parallel)^2_{\min}}{c^2}\right]^{-1/2} - 1, \quad (16)$$

where

$$\frac{(v_\parallel)_{\min}}{c} = \begin{cases} \dfrac{xy - s(1+y^2-x^2)^{1/2}}{1+y^2}, & \sigma = e \\ \dfrac{xy + \varepsilon s(\varepsilon^2+y^2-x^2)^{1/2}}{\varepsilon^2+y^2}, & \sigma = p \end{cases}$$

corresponding to R-mode ($s = 1$) or L-mode ($s = -1$) waves. In each of Figures 3–6, corresponding to the given dispersion curves in the top, we plot the minimum resonant energy curves for electrons in the middle and for protons in the bottom. Figures 3–6 demonstrate that the minimum resonant energy $E_{\min}$ increases as the value of the parameter $\alpha^* = \Omega_e^2/\omega_{pe}^2$ increases. Thus since $\alpha^* \propto B_0^2/N_0$, the value of $E_{\min}$ increases as the background magnetic field B_0 increases or as the electron number density N_0 decreases. Clearly, $E_{\min}$ depends critically on the wave frequency and the local values of B_0 and N_0. Figure 6 also demonstrates that for L-mode waves in a multi-ion plasma the value of $E_{\min}$ can be sensitively dependent on the fractional ion number densities (η_1, η_2, η_3). A detailed examination of the variation of minimum resonant energy with fractional ion composition is given by *Summers and Thorne* [2003].

[13] Formulae (5)–(7) are exact, closed-form expressions for the rates of resonant diffusion $D_{\alpha\alpha}$, $D_{\alpha p}/p$, and D_{pp}/p^2, that can be evaluated as functions of the particle kinetic energy E_k and pitch angle α. Input parameters to be specified are $|\Omega_\sigma|$, $|\Omega_e|$, R, α^*, x_m, δx, and ρ. For a given wave mode and set of input parameters, it is useful to identify the regions in the (E_k, α) - plane over which

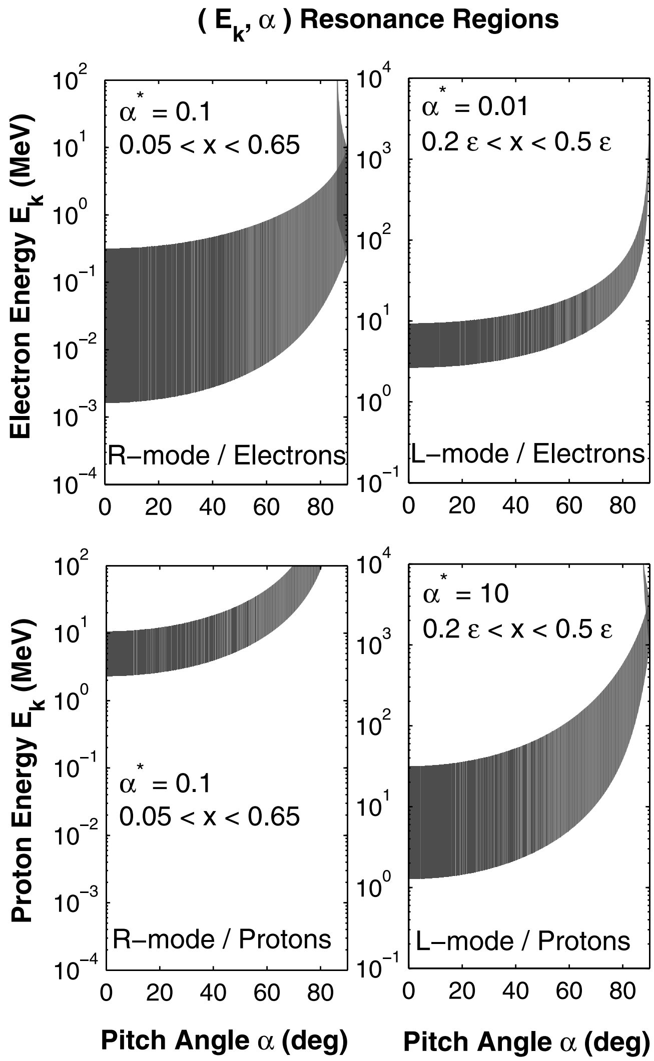

Figure 7. Examples of (E_k, α) resonance regions for the specified wave-particle interactions and the given parameter values.

gyroresonance can take place. We plot examples of such (E_k, α) "resonance regions" in Figure 7. In the top we consider electrons interacting with R-mode or L-mode waves and, in the bottom, protons interacting with R-mode or L-mode waves. The diffusion coefficients (5)–(7) exist within the shaded regions shown in Figure 7 and are zero outside the shaded regions. The extent of the resonance region is generally determined by the particle species, the wave mode, the frequency band $\omega_1 < \omega < \omega_2$, and the value of the parameter $\alpha^* = \Omega_e^2/\omega_{pe}^2$. From the gyroresonance condition (9) we find that the boundary of the (E_k, α) resonance region generally includes the curves,

$$\cos\alpha = \frac{\phi_1 + s\lambda/(E+1)}{\beta\kappa_1}, \quad \cos\alpha = \frac{\phi_2 + s\lambda/(E+1)}{\beta\kappa_2}, \tag{17}$$

where $\beta = [E(E+2)]^{1/2}/(E+1)$, $\phi_1 = \omega_1/|\Omega_e|$, $\kappa_1 = ck_1/|\Omega_e|$, $\phi_2 = \omega_2/|\Omega_e|$, and $\kappa_2 = ck_2/|\Omega_e|$. In Figure 8, for the electron/R-mode wave interaction, we examine the sensitivity of the (E_k, α) resonance region to changes in the α^* - value and the wave frequency band, $\omega_1 < \omega < \omega_2$. In the top we keep the wave band fixed ($0.05 < x < 0.65$), and set the values $\alpha^* = 0.01$ and $\alpha^* = 1$. In the bottom we keep $\alpha^* = 0.1$ and consider the frequency bands $0.1 < x < 0.4$ and $0.1 < x < 0.8$. These figures demonstrate that the (E_k, α) resonance region is sensitively dependent on the assumed values for the α^* - parameter and the wave frequency band.

4. Resonant Wave Frequencies

[14] The wave frequencies $x = \omega/|\Omega_e|$ and wave numbers $y = ck/|\Omega_e|$ that are resonant with a particle of given kinetic energy E and pitch angle α are given by the simultaneous solution of the resonance condition (9) and the dispersion equations (11), for a multi-ion (H^+, He^+, O^+) plasma. The

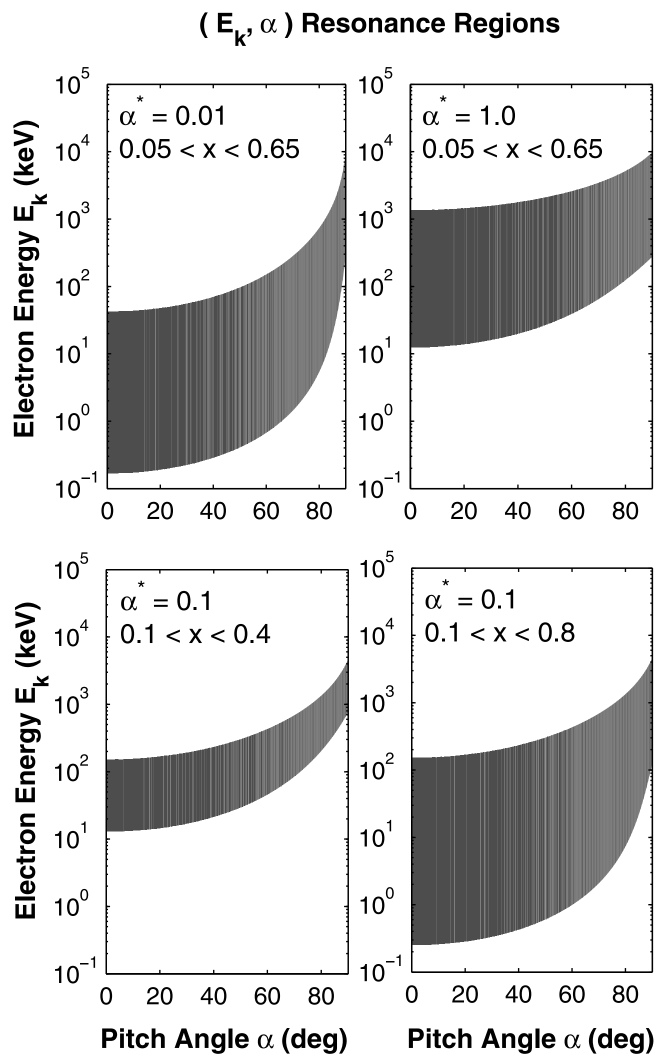

Figure 8. (E_k, α) resonance regions for R-mode/electron interaction. Sensitivity of the resonance region to a change in the value of $\alpha^* = \Omega_e^2/\omega_{pe}^2$, for a fixed frequency band, is tested in the top; sensitivity to a change in the frequency band, for a fixed α^*, is tested in the bottom.

resonant wave frequencies x are found to satisfy the sixth-order polynomial equation,

$$x^6 + A_1 x^5 + A_2 x^4 + A_3 x^3 + A_4 x^2 + A_5 x + A_6 = 0 \quad (18)$$

where

$$\begin{aligned}
A_1 &= [s(84\varepsilon - 64) + 128a + \xi^2 s(64 - 84\varepsilon)]/[64(1 - \xi^2)],\\
A_2 &= [\varepsilon(21\varepsilon - 84) + as(168\varepsilon - 128) + 64a^2 \\
&\quad + \xi^2\varepsilon(84 - 21\varepsilon) + A\xi^2/\alpha^*]/[64(1 - \xi^2)],\\
A_3 &= [s\varepsilon^2(\varepsilon - 21) + a\varepsilon(42\varepsilon - 168) + a^2 s(84\varepsilon - 64)\\
&\quad + \xi^2\varepsilon^2 s(21 - \varepsilon) + B\xi^2/\alpha^*]/[64(1 - \xi^2)],\\
A_4 &= [sa\varepsilon^2(2\varepsilon - 42) + a^2\varepsilon(21\varepsilon - 84) - \varepsilon^3(1 - \xi^2)\\
&\quad + C\xi^2/\alpha^*]/[64(1 - \xi^2)],\\
A_5 &= a\varepsilon^2[as(\varepsilon - 21) - 2\varepsilon]/[64(1 - \xi^2)],\\
A_6 &= -a^2\varepsilon^3/[64(1 - \xi^2)],\\
A &= 64 + \varepsilon[64\eta_1 + 16\eta_2 + 4\eta_3],\\
B &= s\varepsilon[84 - \{(64 - 20\varepsilon)\eta_1 + (16 - 17\varepsilon)\eta_2\\
&\quad + (4 - 5\varepsilon)\eta_3\}],\\
C &= \varepsilon^2[21 - \{(20 - \varepsilon)\eta_1 + (17 - \varepsilon)\eta_2 + (5 - \varepsilon)\eta_3\}],\\
\xi &= \beta \cos\alpha,\ \beta = [E(E + 2)]^{1/2}/(E + 1),\\
a &= s\lambda/\gamma,\ \gamma = E + 1,
\end{aligned}$$

and α^* is defined by (12). The corresponding wave numbers y can be determined from (9). In the special case of a hydrogen plasma ($\eta_1 = 1$, $\eta_2 = 0$, $\eta_3 = 0$), equation (18) can be shown to reduce to a quartic equation, as given by equation (A1) of *Summers* [2005]. This quartic equation alternately follows by eliminating the wave number y from equations (9) and (13).

[15] Since we assume that the wave frequency ω is positive, we seek real resonant roots $x > 0$ in the appropriate frequency range. For $\cos\alpha > 0$, a forward propagating wave corresponds to $y > 0$, and a backward propagating wave to $y < 0$. We identify the following four cases: (1) R-mode waves interacting with electrons ($s = 1$, $\lambda = -1$), (2) L-mode waves interacting with protons ($s = -1$, $\lambda = \varepsilon$), (3) R-mode waves interacting with protons ($s = 1$, $\lambda = \varepsilon$), (4) L-mode waves interacting with electrons ($s = -1$, $\lambda = -1$). For a hydrogen plasma, the roots of interest are in the range $0 < x < 1$ for R-mode waves, and $0 < x < \varepsilon$ for L-mode waves. In the cases 1, 2, and 3, there is a maximum of three relevant roots, while in case 4 there is one relevant root. *Summers* [2005] inadvertently suppressed the possibility that case 3 could permit three relevant roots. We are grateful to R. Gendrin (personal communication, 2006) for emphasizing that three roots are possible in case 3, the R-mode/proton interaction, as discussed, for instance, by *Gintsburg* [1962] and *Gendrin* [1965]. For a multi-ion (H^+, He^+, O^+) plasma, the roots of interest are in the range $\varepsilon/4 < x < \varepsilon$ for L-mode H^+ band waves, $\varepsilon/16 < x < \varepsilon/4$ for the L-mode He^+ band, $0 < x < \varepsilon/16$ for the L-mode O^+ band, and $0 < x < 1$ for R-mode waves. We have carried out numerical experiments to determine the number of relevant roots of equation (18) in the cases 1–4 for a multi-ion plasma. Our numerical experiments imply that (1) in cases 1 and 3, there is a maximum of three relevant roots, and (2) in cases 2 and 4, for each of the H^+, He^+, and O^+ bands, there is one relevant root.

5. Bounce-Averaging

[16] Equations (5)–(7), which have been derived for a uniform background magnetic field, give values for the local rates of diffusion, i.e., at a given point in space. In order to apply (5)–(7) to a magnetic mirror geometry such as the Earth's magnetic field, the diffusion coefficients must be bounce-averaged, i.e., averaged over particle bounce-orbits. The Earth's dipole magnetic field B is given by

$$B = B_{eq} f(\lambda), \quad (19)$$

with

$$f(\lambda) = \frac{\left(1 + 3\sin^2\lambda\right)^{1/2}}{\cos^6\lambda}, \quad (20)$$

where B_{eq} is the equatorial magnetic field, and λ is the magnetic latitude. Constancy of the (first) adiabatic invariant associated with the gyration of a particle about a field line gives

$$\frac{\sin^2\alpha}{B} = \frac{\sin^2\alpha_{eq}}{B_{eq}}, \quad (21)$$

where α is the particle pitch angle at any point along a field line, and α_{eq} is the equatorial pitch angle. Equations (19) and (21) imply that

$$\sin^2\alpha = f(\lambda)\sin^2\alpha_{eq}. \quad (22)$$

In order to carry out bounce-averaging of the diffusion coefficients over a particle bounce-orbit, the local diffusion coefficients must first be related to the equivalent equatorial coefficients [*Roberts*, 1969; *Lyons et al.*, 1972; *Lyons*, 1974]. This is achieved by multiplying $D_{\alpha\alpha}$, $D_{\alpha p}$, and D_{pp}, respectively, by $(\partial\alpha_{eq}/\partial\alpha)^2$, $(\partial\alpha_{eq}/\partial\alpha)$, and 1, where, from (21),

$$\frac{\partial\alpha_{eq}}{\partial\alpha} = \frac{\tan\alpha_{eq}}{\tan\alpha}. \quad (23)$$

The bounce-averaged values of the diffusion coefficients (5)–(7) therefore take the form,

$$\langle D_{\alpha\alpha}\rangle = \mathcal{D}_{\alpha\alpha}\left(\alpha_{eq}\right) = \frac{1}{\tau_B}\int_0^{\tau_B} D_{\alpha\alpha}(\alpha)\left(\frac{\partial\alpha_{eq}}{\partial\alpha}\right)^2 dt, \quad (24)$$

$$\langle D_{\alpha p}\rangle = \mathcal{D}_{\alpha p}\left(\alpha_{eq}\right) = \frac{1}{\tau_B}\int_0^{\tau_B} D_{\alpha p}(\alpha)\left(\frac{\partial\alpha_{eq}}{\partial\alpha}\right) dt \quad (25)$$

$$= \langle D_{p\alpha}\rangle = \mathcal{D}_{p\alpha}\left(\alpha_{eq}\right), \quad (26)$$

$$\langle D_{pp}\rangle = \mathcal{D}_{pp}\left(\alpha_{eq}\right) = \frac{1}{\tau_B}\int_0^{\tau_B} D_{pp}(\alpha)\, dt, \quad (27)$$

where τ_B is the bounce-period of the particle; τ_B can be written in the approximate form,

$$\tau_B = \frac{4R_0 S\left(\alpha_{eq}\right)}{v_0} \quad (28)$$

[*Hamlin et al.*, 1961], where R_0 is the distance from the dipole center to the point at which the field line crosses the equatorial plane, v_0 is the particle speed, and

$$S(\alpha_{eq}) = 1.3 - 0.56 \sin \alpha_{eq}. \qquad (29)$$

[17] It is useful to transform the time-averages (24)–(27) over a bounce-orbit to integrals over the magnetic latitude λ. From the magnetic field line equation $R = R_0 \cos^2 \lambda$, we derive the element of arc length, $dl = R_0 \cos \lambda \, (1 + 3\sin^2 \lambda)^{1/2} d\lambda$. Using also equations (22) and (23), and the relation $dl = v_0 \cos \alpha \, dt$, we obtain from (24)–(27) the results,

$$\langle D_{\alpha\alpha} \rangle = \frac{1}{S(\alpha_{eq})} \int_0^{\lambda_m} D_{\alpha\alpha}(\alpha) \frac{\cos \alpha \cos^7 \lambda}{\cos^2 \alpha_{eq}} d\lambda, \qquad (30)$$

$$\langle D_{\alpha p} \rangle = \langle D_{p\alpha} \rangle = \frac{1}{S(\alpha_{eq})} \int_0^{\lambda_m} D_{\alpha p}(\alpha) \frac{\sin \alpha \cos^7 \lambda}{\sin \alpha_{eq} \cos \alpha_{eq}} d\lambda, \qquad (31)$$

$$\langle D_{pp} \rangle = \frac{1}{S(\alpha_{eq})} \int_0^{\lambda_m} D_{pp}(\alpha) \frac{\sin^2 \alpha \cos^7 \lambda}{\sin^2 \alpha_{eq} \cos \alpha} d\lambda, \qquad (32)$$

where λ_m is the latitude of the mirror point of the particle, given by

$$X^6 + (3 \sin^4 \alpha_{eq}) X - 4 \sin^4 \alpha_{eq} = 0, \qquad (33)$$

with $X = \cos^2 \lambda_m$. Equation (33) is obtained by setting α = 90 deg in equation (22).

[18] In results (30)–(32), α is regarded as a function of α_{eq} and λ, as given by relation (22); thus the bounce-averaged diffusion coefficients $\langle D_{\alpha\alpha} \rangle$, $\langle D_{\alpha p} \rangle$, and $\langle D_{pp} \rangle$ are functions of α_{eq}. To calculate the integrals in (30)–(32), for a given value of α_{eq}, the local diffusion coefficients $D_{\alpha\alpha}$, $D_{\alpha p}$, and D_{pp} must first be evaluated at a set of specified λ-values in the range $0 < \lambda < \lambda_m$. This requires the calculation of the resonant roots (the appropriate solutions of the polynomial equation (18)) at each of the specified λ-values. The integrals in (30)–(32) can then be evaluated by a standard numerical quadrature technique.

[19] In Figure 9 we plot values of the particle mirror latitude λ_m as a function of α_{eq}, as determined by equation (33). We also show in Figure 9 the variation of the function f with magnetic latitude λ, as given by equation (20).

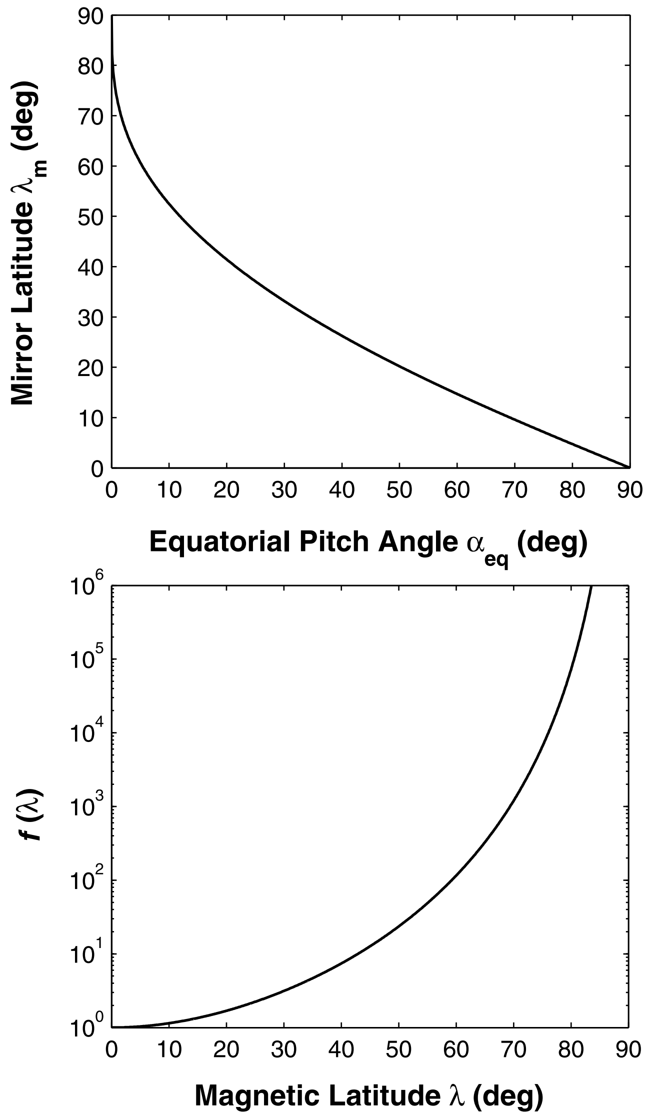

Figure 9. (top) Variation of the particle mirror latitude λ_m with equatorial pitch angle, as specified by (33). (bottom) Variation of the functional value $f(\lambda) = B/B_{eq}$ with magnetic latitude λ, given by (20).

6. Discussion

[20] 1. We have presented formulae for the bounce-averaged quasi-linear (momentum, mixed, and pitch angle) diffusion coefficients for cyclotron resonance with field-aligned electromagnetic waves in a hydrogen or multi-ion (H^+, He^+, O^+) plasma. The formulae are exact, tractable, and fully relativistic. The wave frequency spectrum is assumed to be Gaussian. Evaluation of the diffusion coefficients requires the solution of a sixth-order polynomial equation for the resonant wave frequencies in the case of a multi-ion (H^+, He^+, O^+) plasma, compared to the solution of a fourth-order polynomial equation for a hydrogen plasma. In general, the diffusion rates depend on the wave spectral properties, including the wave amplitude, frequency band, MLT distribution and latitudinal distribution, in addition to the background magnetic field B_0 and the electron number density N_0.

[21] 2. In the companion paper [*Summers et al.*, 2007], we apply the results derived here to the interaction of radiation belt electrons with (1) R-mode VLF chorus waves outside the plasmasphere, (2) R-mode ELF hiss inside the plasmasphere, and (3) L-mode EMIC waves inside the plasmasphere. Timescales for electron acceleration or momentum diffusion can be found by using (32) to evaluate $\langle D_{pp} \rangle / p^2$ as a function of equatorial pitch angle, for an electron of a given energy, at a particular L shell. To estimate the electron loss timescale τ_{loss} for a specific wave mode, we determine the quantity $\tau_{loss} = 1/\langle D_{\alpha\alpha} \rangle$, where

$\langle D_{\alpha\alpha} \rangle$ is the bounce-averaged pitch angle diffusion coefficient (given by (30)) for the specified wave band, evaluated at $\alpha_{eq} = (\alpha_L)_{eq}$ where $(\alpha_L)_{eq}$ is the equatorial loss cone angle given by

$$\sin(\alpha_L)_{eq} = \left[L^5(4L-3)\right]^{-1/4}. \quad (34)$$

[22] 3. While the diffusion coefficients presented in this paper have been derived on the assumption of field-aligned wave propagation, this assumption need not unduly restrict the applicability of our results. In some cases, first-order-harmonic diffusion rates can give a valuable approximation to diffusion rates for oblique waves calculated using higher-order resonances. For instance, first-order-harmonic pitch angle diffusion rates for EMIC waves calculated by *Summers and Thorne* [2003] agree well with corresponding higher-order calculations by *Albert* [2003] for oblique waves with wave-normal angle of 25. In another example, *Thorne et al.* [2005b] found that MeV electron scattering rates near the loss cone, due to chorus, agreed within a factor of 2 with calculations from a diffusion code employing ±5 harmonic resonances. This approximate agreement is acceptable for the determination of electron lifetimes since in the study of *Thorne et al.* [2005b] there is a larger uncertainty in the observed lifetimes and in the properties of the waves. In an associated study, *Shprits et al.* [2006b] compared bounce-averaged energy and pitch angle diffusion coefficients for field-aligned chorus waves with calculations for oblique waves that take account of higher-order resonances. *Shprits et al.* [2006b] found that errors associated with the neglect of higher-order scattering are smaller than the inaccuracies associated with uncertainties in the input values of the plasma density and latitudinal distribution of the waves.

[23] 4. Evaluation of bounce-averaged diffusion coefficients for field-aligned electromagnetic waves can typically be carried out in minimal CPU time. Incorporation of diffusion coefficients for field-aligned waves into a radiation belt code is evidently practicable from the point of view of CPU time efficiency. Further, as discussed in paragraph 3 above, errors associated with the omission of higher-order scattering effects may be smaller than inaccuracies associated with uncertainties in input parameter values in the code.

[24] **Acknowledgments.** This work is supported by the Natural Sciences and Engineering Research Council of Canada under grant A-0621.
[25] Zuyin Pu thanks Reiner Friedel and Sebastien Bourdarie for their assistance in evaluating this paper.

References

Albert, J. M. (2003), Evaluation of quasi-linear diffusion coefficients for EMIC waves in a multispecies plasma, *J. Geophys. Res.*, *108*(A6), 1249, doi:10.1029/2002JA009792.

Baker, D. N. (2001), Satellite anomalies due to space storms, in *Space Storms and Space Weather Hazards*, edited by I. A. Daglis, p. 251, Springer, New York.

Baker, D. N. (2002), How to cope with space weather, *Science*, *297*(5586), 1486.

Baker, D. N., J. B. Blake, R. W. Klebesadel, and P. R. Higbie (1986), Highly relativistic electrons in the Earth's outer magnetosphere: 1. Lifetimes and temporal history 1979–1984, *J. Geophys. Res.*, *91*, 4265.

Baker, D. N., J. B. Blake, L. B. Callis, J. R. Cummings, D. Hovestadt, S. G. Kanekal, B. Blecker, R. A. Mewaldt, and R. D. Zwickl (1994), Relativistic electron acceleration and decay timescales in the inner and outer radiation belts: SAMPEX, *Geophys. Res. Lett.*, *21*, 409.

Baker, D. N., et al. (1997), Recurrent geomagnetic storms and relativistic electron enhancements in the outer magnetosphere: ISTP coordinated measurements, *J. Geophys. Res.*, *102*, 14,141.

Baker, D. N., J. H. Allen, S. G. Kanekal, and G. D. Reeves (1998), Disturbed space environment may have been related to pager satellite failure, *Eos Trans. AGU*, *79*, 477.

Callis, L. B., M. Natarajan, J. D. Lambeth, and D. N. Baker (1998), Solar atmospheric coupling by electrons (SOLACE): 2. Calculated stratospheric effects of precipitating electrons, *J. Geophys. Res.*, *103*, 28,421.

Elkington, S. R., M. K. Hudson, and A. A. Chan (2003), Resonant acceleration and diffusion of outer zone electrons in an asymmetric geomagnetic field, *J. Geophys. Res.*, *108*(A3), 1116, doi:10.1029/2001JA009202.

Friedel, R. H. W., G. D. Reeves, and T. Obara (2002), Relativistic electron dynamics in the inner magnetosphere - A review, *J. Atmos. Sol. Terr. Phys.*, *64*, 265.

Gendrin, R. (1965), Gyroresonance radiation produced by proton and electron beams in different regions of the magnetosphere, *J. Geophys. Res.*, *70*, 5369.

Gendrin, R. (2001), The role of wave particle interactions in radiation belts modeling, in *Sun-Earth Connection and Space Weather*, vol. 75, edited by M. Candidi, M. Storini, and U. Villante, p. 151, It. Phys. Soc., Bologna.

Gintsburg, M. A. (1962), Anomalous Doppler effect in a plasma, *Soviet Phys. JETP*, *14*(3), 542.

Green, J. C., and M. G. Kivelson (2004), Relativistic electrons in the outer radiation belt: Differentiating between acceleration mechanisms, *J. Geophys. Res.*, *109*, A03213, doi:10.1029/2003JA010153.

Green, J. C., T. P. O'Brien, T. G. Onsager, B. J. Fraser, H. J. Singer, S. G. Kanekal, D. N. Baker, and R. F. Friedel (2005), A review of the processes which deplete radiation belt electron flux, paper presented at Workshop on Energetic Electron Radiation Belt Dynamics, Hermanus Magn. Obs., Hermanus, South Africa.

Hamlin, D. A., R. Karplus, R. C. Vik, and K. M. Watson (1961), Mirror and azimuthal drift frequencies for geomagnetically trapped particles, *J. Geophys. Res.*, *66*, 1.

Horne, R. B. (2002), The contribution of wave-particle interactions to electron loss and acceleration in the Earth's radiation belts during geomagnetic storms, in *Review of Radio Science 1999–2002*, edited by W. R. Stone, chap. 33, pp. 801–828, John Wiley, Hoboken, N. J.

Horne, R. B., and R. M. Thorne (2003), Relativistic electron acceleration and precipitation during resonant interactions with whistler-mode chorus, *Geophys. Res. Lett.*, *30*(10), 1527, doi:10.1029/2003GL016973.

Horne, R. B., R. M. Thorne, S. A. Glauert, J. M. Albert, N. P. Meredith, and R. R. Anderson (2005a), Timescale for radiation belt electron acceleration by whistler mode chorus waves, *J. Geophys. Res.*, *110*, A03225, doi:10.1029/2004JA010811.

Horne, R. B., et al. (2005b), Wave acceleration of electrons in the Van Allen radiation belts, *Nature*, *437*, 227, doi:10.1038/nature03939.

Hudson, M. K., S. R. Elkington, J. G. Lyon, M. J. Wiltberger, and M. Lessard (2001), Radiation belt electron acceleration by ULF wave drift resonance: Simulation of 1997 and 1998 storms, in *Space Weather*, *Geophys. Monogr. Ser.*, vol. 125, edited by P. Song, H. J. Singer, and G. L. Siscoe, p. 289, AGU, Washington, D. C.

Iles, R. H. A., N. P. Meredith, A. N. Fazakerley, and R. B. Horne (2006), Phase space density analysis of the outer radiation belt energetic electron dynamics, *J. Geophys. Res.*, *111*, A03204, doi:10.1029/2005JA011206.

Lastovicka, J. (1996), Effects of geomagnetic storms in the lower ionosphere, middle atmosphere and troposphere, *J. Atmos. Terr. Phys.*, *58*, 831.

Li, X., and M. A. Temerin (2001), The electron radiation belt, *Space Sci. Rev.*, *95*, 569.

Li, X., D. N. Baker, M. A. Temerin, T. E. Cayton, E. G. D. Reeves, R. A. Christensen, J. B. Blake, M. D. Looper, R. Nakamura, and S. G. Kanekal (1997), Multi-satellite observations of the outer zone electron variation during the November 3–4, 1993, magnetic storm, *J. Geophys. Res.*, *102*, 14,123.

Lyons, L. R. (1974), Electron diffusion driven by magnetospheric electrostatic waves, *J. Geophys. Res.*, *79*, 575.

Lyons, L. R., R. M. Thorne, and C. F. Kennel (1972), Pitch-angle diffusion of radiation belt electrons within the plasmasphere, *J. Geophys. Res.*, *77*, 3455.

Melrose, D. B. (1980), *Plasma Astrophysics*, vol. 2, *Nonthermal Processes in Diffuse Magnetized Plasmas*, Gordon and Breach, New York.

Meredith, N. P., R. B. Horne, S. A. Glauert, R. M. Thorne, D. Summers, J. M. Albert, and R. R. Anderson (2006), Energetic outer zone electron loss timescales during low geomagnetic activity, *J. Geophys. Res.*, *111*, A05212, doi:10.1029/2005JA011516.

Miyoshi, Y., and R. Kataoka (2005), Ring current ions and radiation belt electrons during geomagnetic storms driven by coronal mass ejections and corotating interaction regions, *Geophys. Res. Lett.*, *32*, L21105, doi:10.1029/2005GL024590.

Miyoshi, Y., A. Morioka, T. Obara, H. Misawa, T. Nagai, and Y. Kasahara (2003), Rebuilding process of the outer radiation belt during the 3 November 1993 magnetic storm: NOAA and Exos-D observations, *J. Geophys. Res.*, *108*(A1), 1004, doi:10.1029/2001JA007542.

Miyoshi, Y., V. K. Jordanova, A. Morioka, and D. S. Evans (2004), Solar cycle variations of the electron radiation belts: Observations and radial diffusion simulation, *Space Weather*, *2*, S10S02, doi:10.1029/2004SW000070.

Obara, T., M. Den, Y. Miyoshi, and A. Morioka (2000), Energetic electron variation in the outer radiation zone during the early May 1998 magnetic storm, *J. Atmos. Sol. Terr. Phys.*, *62*, 1405.

O'Brien, T. P., K. R. Lorentzen, I. R. Mann, N. P. Meredith, J. B. Blake, J. F. Fennell, M. D. Looper, D. K. Milling, and R. R. Anderson (2003), Energization of relativistic electrons in the presence of ULF power and MeV microbursts: Evidence for dual ULF and VLF acceleration, *J. Geophys. Res.*, *108*(A8), 1329, doi:10.1029/2002JA009784.

Paulikas, G. A., and J. B. Blake (1979), Effects of the solar wind on magnetospheric dynamics: Energetic electrons at synchronous orbit, in *Quantitative Modeling of Magnetospheric Processes*, *Geophys. Monogr. Ser.*, vol. 21, edited by W. P. Olsen, p. 180, Washington D. C.

Reeves, G. D., R. H. W. Friedel, R. D. Belian, M. M. Meiet, M. G. Henderson, T. Onsager, H. J. Singer, D. N. Baker, X. Li, and J. B. Blake (1998), The relativistic electron response at geosynchronous orbit during the January 1997 magnetic storm, *J. Geophys. Res.*, *103*, 17,559.

Roberts, C. S. (1969), Pitch-angle diffusion of electrons in the magnetosphere, *Rev. Geophys.*, *7*, 305.

Roth, I., M. Temerin, and M. K. Hudson (1999), Resonant enhancement of relativistic electron fluxes during geomagnetically active periods, *Ann. Geophys.*, *17*, 631.

Sheeley, B. W., M. B. Moldwin, H. K. Rassoul, and R. R. Anderson (2001), An empirical plasmasphere and trough density model: CRRES observations, *J. Geophys. Res.*, *106*, 25,631.

Shprits, Y. Y., and R. M. Thorne (2004), Time dependent radial diffusion modeling of relativistic electrons with realistic loss rates, *Geophys. Res. Lett.*, *31*, L08805, doi:10.1029/2004GL019591.

Shprits, Y. Y., R. M. Thorne, R. B. Horne, S. A. Glauert, M. Cartwright, C. T. Russell, D. N. Baker, and S. G. Kanekal (2006a), Acceleration mechanism responsible for the formation of the new radiation belt during the 2003 Halloween solar storm, *Geophys. Res. Lett.*, *33*, L05104, doi:10.1029/2005GL024256.

Shprits, Y. Y., R. M. Thorne, R. B. Horne, and D. Summers (2006b), Bounce-averaged diffusion coefficients for field-aligned chorus waves, *J. Geophys. Res.*, *111*, A10225, doi:10.1029/2006JA011725.

Stix, T. H. (1992), *Waves in Plasmas*, Am. Inst. of Phys., New York.

Summers, D. (2005), Quasi-linear diffusion coefficients for field-aligned electromagnetic waves with applications to the magnetosphere, *J. Geophys. Res.*, *110*, A08213, doi:10.1029/2005JA011159.

Summers, D., and C. Ma (2000), A model for generating relativistic electrons in the Earth's inner magnetosphere based on gyroresonant wave-particle interactions, *J. Geophys. Res.*, *105*, 2625.

Summers, D., and R. M. Thorne (2003), Relativistic electron pitch angle scattering by electromagnetic ion cyclotron waves during geomagnetic storms, *J. Geophys. Res.*, *108*(A4), 1143, doi:10.1029/2002JA009489.

Summers, D., R. M. Thorne, and F. Xiao (1998), Relativistic theory of wave-particle resonant diffusion with application to electron acceleration in the magnetosphere, *J. Geophys. Res.*, *103*, 20,487.

Summers, D., C. Ma, N. P. Meredith, R. B. Horne, R. M. Thorne, D. Heynderickx, and R. R. Anderson (2002), Model of the energization of outer-zone electrons by whistler-mode chorus during the October 9, 1990 geomagnetic storm, *Geophys. Res. Lett.*, *29*(4), 2174, doi:10.1029/2002GL016039.

Summers, D., C. Ma, and T. Mukai (2004a), Competition between acceleration and loss mechanisms of relativistic electrons during geomagnetic storms, *J. Geophys. Res.*, *109*, A04221, doi:10.1029/2004JA010437.

Summers, D., C. Ma, N. P. Meredith, R. B. Horne, R. M. Thorne, and R. R. Anderson (2004b), Modeling outer-zone relativistic electron response to whistler-mode chorus activity during substorms, *J. Atmos. Sol. Terr. Phys.*, *66*, 133.

Summers, D., R. L. Mace, and M. A. Hellberg (2005), Pitch-angle scattering rates in planetary magnetospheres, *J. Plasma Phys.*, *71*(3), 237.

Summers, D., B. Ni, and N. P. Meredith (2007), Timescales for radiation belt electron acceleration and loss due to resonant wave-particle interactions: 2. Evaluation for VLF chorus, ELF hiss, and electromagnetic ion cyclotron waves, *J. Geophys. Res.*, *112*, A04207, doi:10.1029/2006JA011993.

Thorne, R. M., R. B. Horne, S. A. Glauert, N. P. Meredith, Y. Shprits, D. Summers, and R. R. Anderson (2005a), The influence of wave-particle interactions on relativistic electron dynamics during storms, in *Inner Magnetosphere Interactions: New Perspectives From Imaging*, *Geophys. Monogr. Ser.*, vol. 159, edited by J. Burch, M. Schulz, and H. Spence, p. 101, AGU, Washington, D. C.

Thorne, R. M., T. P. O'Brien, Y. Y. Shprits, D. Summers, and R. B. Horne (2005b), Timescale for MeV electron microburst loss during geomagnetic storms, *J. Geophys. Res.*, *110*, A09202, doi:10.1029/2004JA010882.

Varotsou, A., D. Boscher, S. Bourdarie, R. B. Horne, S. A. Glauert, and N. P. Meredith (2005), Simulation of the outer radiation belt electrons near geosynchronous orbit including both radial diffusion and resonant interaction with whistler-mode chorus waves, *Geophys. Res. Lett.*, *32*, L19106, doi:10.1029/2005GL023282.

N. P. Meredith, British Antarctic Survey, Natural Environment Research Council, Madingley Road, Cambridge, CB3 0ET, UK. (nmer@bas.ac.uk)

B. Ni and D. Summers, Department of Mathematics and Statistics, Memorial University of Newfoundland, St. John's, Newfoundland, Canada A1C 5S7. (bbni@math.mun.ca; dsummers@math.mun.ca)